



Transparent solar photovoltaic windows provide a strong potential for self-sustainable food production in forward-looking greenhouse farming architectures

Hao Luo ^a , Mikhail Vasiliev ^b, Tianhua He ^a, Penghao Wang ^a , Jamie Lyford ^b, Victor Rosenberg ^b, Chengdao Li ^{a,*} 

^a Western Crop Genetics Alliance, Murdoch University, 90 South Street, Murdoch, WA 6150, Australia

^b ClearVue Technologies Limited, Suite 7/567 Newcastle Street, West Perth, WA 6005, Australia

ARTICLE INFO

Keywords:

Solar greenhouse
Sustainability
Greenhouse farming
Carbon neutrality

ABSTRACT

Agriculture is a major contributor to global environmental challenges and is highly vulnerable to climate change. High-technology greenhouse farming provides efficient, secure and climate-resilient food production but costs significant energy to operate. We designed and constructed a greenhouse with high-transparency photovoltaic windows used as roof- and wall-mounted components of building envelope and demonstrated its significant potential to improve the sustainability of greenhouse farming. This innovative structure reduced energy consumption by 57% and water usage by 29% in research-scale greenhouse production. We showed that several crops commonly produced in greenhouses exhibited no yield loss when grown in solar greenhouses, including tomato, snow pea, spinach mustard, dwarf bean, bell pepper and lettuce. Due to a limitation in the experimental design, solar windows were not fully installed on the greenhouse, which led to an underestimation of the potential energy savings. A computing model showed that a fully glazed solar greenhouse has the potential to offset up to 100% of the energy consumption in worldwide locations by using adaptable and efficient temperature control techniques, thereby potentially enabling completely self-sustainable greenhouse farming on a global scale. The potential of self-sustainable greenhouse farming could be further enhanced by refining its wavelength-selective transmittance and using genetic manipulation to engineer crops that thrive in the solar greenhouse environment. The solar greenhouse technology represents significant opportunities to make substantial progress towards achieving net-zero emissions in global food systems by 2050.

Nomenclature

Symbol	Meaning
OSCs	semitransparent organic solar cells
PAR	photosynthetically active radiation
PPFD	photosynthetic photon flux density
SAS	shade-avoidance syndromes
Φ PSII	actual quantum yield of PSII in light-adapted leaves
Fv/Fm	maximum quantum efficiency of photosystem II
ETR	electron transport rate
ROI	return on investment
UV	ultraviolet
P_{max}	electric power outputs
HVAC	heating, ventilation, and air conditioning system
E_{grid_normal}	electricity imported from the grid in normal room

(continued on next column)

(continued)

Symbol	Meaning
E_{grid_solar}	electricity imported from the grid in solar room
g_{sw}	Stomatal conductance to water
W_{fresh}	plant fresh biomass
W_{dry}	plant dry biomass

1. Introduction

Agriculture has posed significant challenges to the environment worldwide: claiming up to 85% of human water consumption (Djevic and Dimitrijevic, 2009), emitting around 25% of the global greenhouse

* Corresponding author.

E-mail address: C.Li@murdoch.edu.au (C. Li).

gas, clearing grassland and forest for farms but in the meantime (Costa et al., 2022), losing more than a third of existing arable land in past decades (Laborde et al., 2021; Golasa et al., 2021; Panchasara et al., 2021). Climate change, especially the frequent droughts and other extreme weather events poses serious challenges to sustainable agricultural production in conventional farming systems. High-technology greenhouse farming has gained considerable attention and is being scaled up in recent years, as it increases land use efficiency, protects crops from extreme weather, reduces water consumption, and extends growing seasons (Calicioglu et al., 2019). However, high-technology greenhouse farming requires significant energy consumption. For instance, approximately 1.5% of Europe's total energy consumption is attributed to the heating and cooling of commercial greenhouses (Paris et al., 2022). In United States, the electricity consumption for indoor cannabis production ranges from 1817 to 4576 kWh kg⁻¹ of flower produced annually (Summers et al., 2021). This dramatic rise in energy consumption escalates production costs and produces substantial carbon dioxide emissions, increasing environmental pressures. Innovations optimizing renewable energy generation and energy use are thus urgently needed in agricultural production systems to achieve net-zero emissions in global food systems by 2050 (Costa et al., 2022).

To overcome this challenge and establish an environmentally sustainable greenhouse farming system, a new trend has emerged to integrate high-transparency solar windows into greenhouse structures. Gavrilă and Gontean initially proposed this concept in 2010 (Gavrilă and Gontean, 2010), and in recent years, several prototypes of high-transparency photovoltaic modules have been developed (Yano et al., 2014; Li et al., 2018; Cossu et al., 2016). Solar greenhouses with rooftop-mounted high-transparency photovoltaic modules use a portion of the captured sunlight to generate electricity by the solar cells while allowing the remaining sunlight to pass through into the greenhouse for plant growth and food production, representing an energy innovation in modern greenhouse farming systems. Following the initial development of prototype modules, several studies have focused on creating transparent solar panels with varying transmittance levels for greenhouse applications, such as semitransparent organic solar cells (OSCs) with a transmittance around 35% (Ravishankar et al., 2020, 2021) and tinted semi-transparent solar panels with a transmittance around 43% (Thompson et al., 2020). However, at present stage, there has been no practical implementation of a fully operational solar greenhouse to assess its actual energy consumption, power generation capabilities, and crop production potential. Recently, breakthroughs in novel glass products allowing thermal energy savings and solar energy harvesting by patterned-semiconductor thin-film energy converters on glass substrates have demonstrated the capacity of visible light transmission with significant electric power outputs (Vasiliev et al., 2023a), which makes it possible for farming production in self-sustainable solar greenhouses with rooftop-mounted high-transparency photovoltaic modules. In this study, we designed and constructed a research-scale greenhouse with high-transparency photovoltaic modules used as construction materials for roof and windows. The key aims of this project were as follows: 1) monitor the energy consumption and generation in a practical solar greenhouse and estimate the efficiency of electricity offset; 2) develop and establish a self-sustainable greenhouse food production system; 3) comprehensively evaluate the food production capacity in the clear solar greenhouse rooms with different PVB interlayers and compare them to a conventional greenhouse; 4) provide insights addressing existing challenges in this self-sustainable food production system for future improvement. This research addresses a critical research gap, providing valuable insights into the feasibility and sustainability of solar greenhouses as a transformative solution for modern agriculture.

2. Methods

2.1. ClearVue solar greenhouse

ClearVue Technologies developed a high-transparency PV glass product, designed through the innovative application of advanced glazings using fluorescent concentrator panels, spectrally selective thin-film coatings and custom-designed silicon-based solar cell modules. These highly transparent PV glass glazing systems mainly used ultraviolet (UV), violet-blue, and infrared radiation energy to enable a partial redirection of the incoming solar energy towards PV cell surfaces. They had direct VLT at around 60% and total (direct plus diffused) VLT at around 70%, with significant power conversion efficiency (about 3.3%) measured in the glazing-integrated large-area PV window modules with electric power outputs (P_{max}) of 30–33 W_p/m² (17). More information about this product, including interlayers, coatings and its core technologies, was described previously (Vasiliev et al., 2023a, 2023b; Alghamedi et al., 2014).

A research-scale clear solar agrivoltaic greenhouse was constructed at Murdoch University (Fig. 1) (32°04'24.7"S and 115°50'17.2"E) by using ClearVue high-transparency PV windows with functional custom-designed interlayer materials and electric circuitry to generate renewable energy for its operation. The greenhouse is laid out in the east/west orientation along its length, to ensure a higher overall illumination capture of solar energy and thermal efficiency, especially in winter. There were four growth rooms. Room 1 was glazed with conventional low-iron (ultra-clear) glass, and Rooms 2, 3 and 4 with solar glasses. The solar glasses used in Rooms 2, 3 and 4 had minor differences in the formulations of their fluorescent particle-loaded PVB interlayers and the order in which they were arranged within their central panes. Two types of PVB designs were used, including PVB-1, a lower doping concentration for higher-clarity windows, and PVB-2, slightly higher luminescent particle concentration, resulting in slightly higher haze. Despite the differences in doping, no significant visual clarity differences were observed due to the low concentrations of functional materials. The interlayer configurations were as follows: room 2 with two identical "PVB-2" interlayers (higher-haze); room 3 with a combination of "PVB-2" and "PVB-1" interlayers; room 4 with a single "PVB-1" interlayer paired with an ordinary PVB interlayer. The detailed differences in PV configurations in rooms 2 to 4 were described in a previous publication (Vasiliev et al., 2023a). The experimental design included distinct grow rooms with various glass types, in order to test the plants productivity versus the glazing type used, and consequently, versus the light intensity and spectral distributions transmitted through different glazing structures. This was tested simultaneously with the variations in the energy harvesting behaviors measured in solar window glazing of slightly different design types (Vasiliev et al., 2023a). For each grow room, the 20-degree tilted north-facing roof and north-facing front windows were fitted with conventional glasses (Room 1) or clear solar glasses (Rooms 2 to 4). The east end of the greenhouse was installed with conventional glasses, and the west end with solar glasses. A total of 153 clear solar windows were installed in the greenhouse. Each greenhouse room was about 8 m long × 6 m wide with 10 growing benches. The growth rooms were separated with solid white walls to prevent light contamination from neighboring rooms. The east and west ends of the greenhouse were also insulated to block extra sunlight from the sides and allow the four grow rooms to receive consistent irradiation intensity from the outdoors.

A heating, ventilation, and air conditioning (HVAC) system coupled with Home Assistant software (<https://www.home-assistant.io/>) and temperature/humidity sensors was configured to keep the temperature within 24 ± 2 °C during the daytime and 18 ± 2 °C at night in all four rooms. The electricity consumption and production of the solar greenhouse were monitored using an electricity meter, which recorded the solar power produced and the electricity imported from grid for each single room. In the daytime, the PV-generated electricity was mainly self-consumed (at >70% rate of self-consumption) to operate the fans,

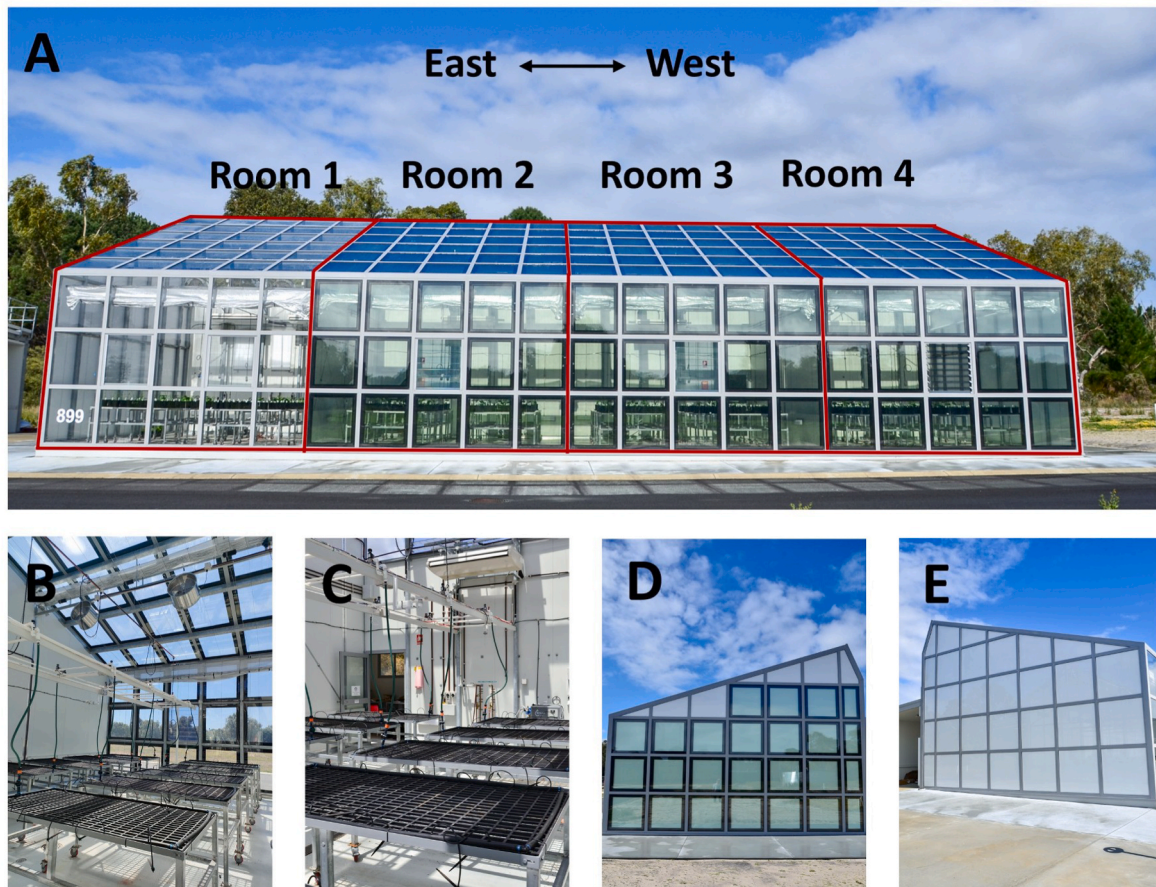


Fig. 1. ClearVue solar greenhouse built at Murdoch University's new Grains Research Precinct. A: Four growth rooms: Rooms 1, 2, 3 and 4 from east (left) to west (right). Room 1 was constructed using conventional glass. Rooms 2 to 4 were constructed with clear solar windows. B: Grow benches and front windows inside a solar glass room. C: Backwall and air-conditioner inside a solar glass room; D: The west end of the greenhouse was constructed with clear solar windows; E: The East end of the greenhouse was constructed with conventional glass panels.

air-conditioners, shades, and ventilation louvres. Extra PV-generated energy was also exported to the electricity grid. At night, the greenhouse operation relied on electricity from the grid. The electricity generated from the solar greenhouse and the energy used to maintain its daily operation were continuously data-logged throughout 2021–2022. The conventional glass room did not produce electricity, so the electricity imported from the grid ($E_{\text{grid_normal}}$) was equal to the total energy consumption. In contrast, the solar glass rooms generated electricity to partially support their own operations. Therefore, for the solar glass rooms, the electricity imported from the grid ($E_{\text{grid_solar}}$) was equal to the total energy consumption minus the energy produced by the solar glass. The energy offset was calculated using the formula: $\text{energy offset} = (E_{\text{grid_normal}} - E_{\text{grid_solar}}) / E_{\text{grid_normal}}$. This formula quantifies the reduction in grid electricity usage due to the energy produced by the solar glass rooms. More details regarding greenhouse construction, microclimate control, electricity production and energy harvesting trends were described in recent publications (Vasiliev et al., 2023a; Moor et al., 2022).

2.2. Water consumption

To assess and compare the daily water consumption, lettuce (variety Green Cos) was cultivated in growing pots in both the normal glass room (Room 1) and the solar glass room (Room 2) in March 2022. The highest daytime temperature was from 34 °C to 38 °C, and lowest at 9 °C at night in this month (Extended Data Table 1 and website <https://www.timeanddate.com/>). The ML3 ThetaProbe Soil Moisture Sensors from

Delta-T Devices were used to monitor soil moisture levels. The initial soil moisture in all pots was adjusted to approximately 25%, and the weights of the pots were recorded. After three days (72 h), the soil moisture levels were measured again, and the difference in weight for each pot was calculated to estimate the amount of water consumed during these three days. To ensure the reliability and consistency of the results, this experiment was carried out with six replicates and repeated three times.

2.3. The light test

The light intensity and quality were tested in each growth room and outdoors using two HOPOOCOLOR OHSP-350 spectrometers (350 nm–800 nm). The light test was done at a sunny midday. One spectrometer was used to measure outdoors, and at the same time, the other spectrometer was used to record light data at the same position on a central bench within each growth room. The spectrometer was set as below: save mode auto; test interval 3s; wavelength range 350 nm–800 nm. The spectrometer had a sensor with a flat surface, so it mainly detected the direct transmittance and might underestimate the diffused transmittance.

2.4. Plant experiment and layout

Crops were grown in the solar greenhouse in two growing seasons. Growing season 1 was from July to December 2021, and growing season 2 was from March to September 2022. The crops, their scientific names, varieties, and sources are listed in Extended Data Table 2, including

horticultural crops commonly produced in greenhouse farming and broadacre crops. Strawberry, lettuce, tomato, dwarf bean, spinach, mustard, basil, snow pea, chili, and bell pepper were selected for this study due to their common use in commercial greenhouse farming. Some of these crops, such as lettuce and tomato, are well-established for their growing conditions in greenhouse environments. On the other hand, wheat, barley, canola, lupin, chickpea, ginger, sunflower, and sweet corn were included because they are either broadacre crops or economically significant. While these crops are not typically grown commercially in greenhouses, they are widely cultivated for research purposes, particularly in breeding programs. In addition to supporting commercial farming, solar greenhouses also have the potential to extend their applications to breeding facilities. This potential to accommodate a diverse range of crops for research and development opens up new possibilities for enhancing agricultural productivity and sustainability. Strawberry was grown from young seedlings, and ginger was grown from a rhizome. The rest of the crops were all grown from seeds. Each crop had 12 replicate pots in a grow room. Each grow pot [180 mm (Tag Lock) Standard Pot, GCP #P180SL] contained 1.7 kg dried Uni Field Station Mix (Richgro, #DE100) and an equal amount of Osmocote Pro 3–4-month (25 kg) NPK (Elemental – 19-3.9-8.3 + 1.2 Mg + TE). The pots were watered evenly by an automatic irrigation system. The plant experiment room layout is shown in Extended Data Fig. 1, and the layout was kept the same in four growth rooms throughout the experiment. To minimize the position effect of light intensity variance, the replicates of each crop were grown on different benches and in different positions in a room. All the benches were rotated clockwise in the rooms once a week to further randomize any position-dependent effects. The experimental design was also illustrated in Extended Data Fig. 2.

2.5. Crops agronomic/physiological traits and yield

The crop seeds were sowed in the pots, and the germination speed (days to emerge) and rate were recorded. The seedling growth data, including seedling height, leaf size and hypocotyl length, were collected around week 3 to week 4. Vegetative development stages and flowering time were recorded based on daily observation throughout the seasons. The vegetative growth data, including plant height, leaf number, size, tiller number, and stem diameter, were collected at flowering time or when harvested. The leaf area was calculated by using Image J software (U.S. National Institutes of Health, <http://rsb.info.nih.gov/ij/download.html>).

The data of photosynthesis characters were collected around flowering time. The chlorophyll content was measured using the atLEAF CHL PLUS chlorophyll meter (FT Green LLC®, USA). For each pot, three mature leaves were selected, and three replicates were measured for the chlorophyll content of each leaf. A LI-600 porometer/fluorometer (LI-COR Biosciences, Lincoln, NE, United States) was used to measure the maximum quantum efficiency of photosystem II (PSII) photochemistry (Fv/Fm) at night. For each pot, three mature leaves were measured for Fv/Fm by instrument settings as below: auto mode fluorescence fast preset (stability limit 5/s; period 2s); flow rate 150 μmol/s; flash dark-adapted, flash intensity 6000 μmol/m²/s, flash length 800 ms; leaf absorbance (abs) 0.84, fraction of absorbance (PS2/1) 0.5; actinic modulation rate 5 Hz. The actual quantum yield of PSII in light-adapted leaves (ΦPSII), photosynthetic electron transport rate (ETR), stomatal conductance to water (g_{sw}) and transpiration rate were also measured by the LI-600 porometer/fluorometer at sunny midday. Three mature leaves were selected and measured for each pot using the settings below: auto mode gsw fast preset (stability limit 0.005 mol/m²/s/s; period 2 s),

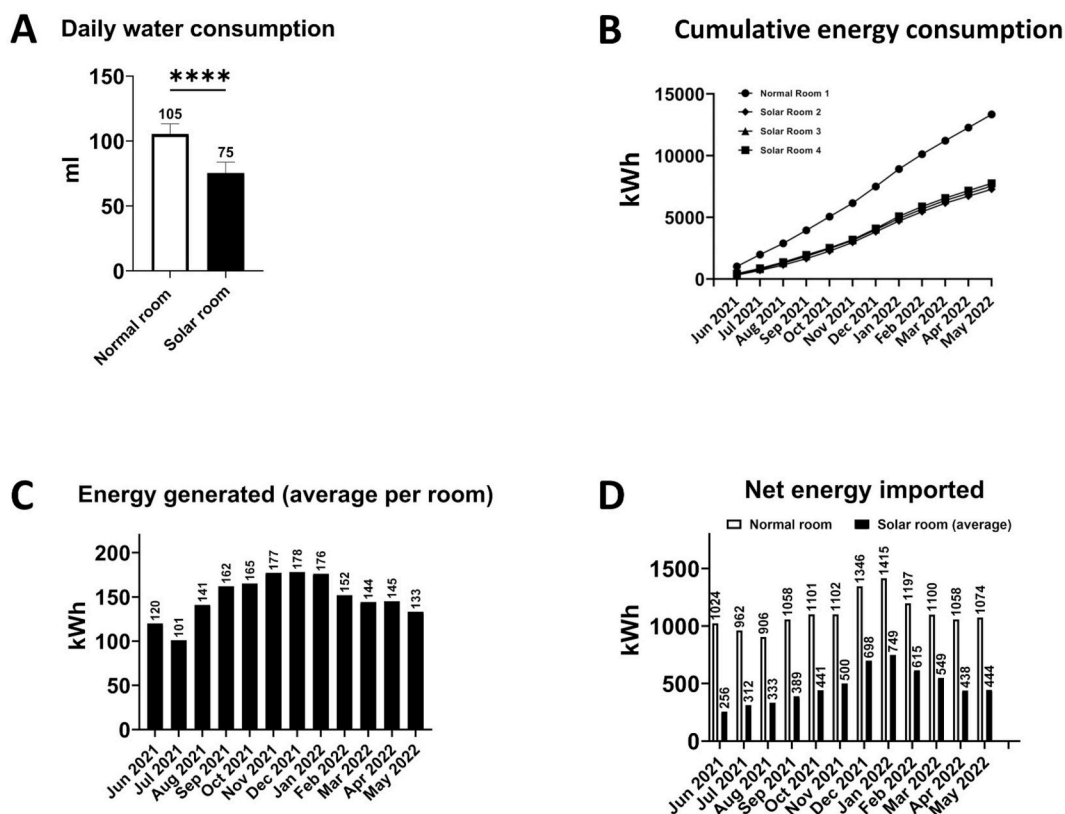


Fig. 2. Water and energy consumption in solar greenhouse and standard greenhouse. A: comparing the average daily water usage of each lettuce pot in conventionally glazed room and solar room; B: comparing cumulative total electricity consumption (grid imported plus solar generated) in normal room and solar room during a one-year period (from June 2021 to May 2022); C: comparing the average solar power generated in different months in a one-year period; D: comparing the net electricity imported from grid (If the energy production from the greenhouse’s solar systems is insufficient to cover its total energy consumption, the deficit must be compensated by importing energy from the grid) in normal room and solar room in a one-year period.

fluorescence fast preset (stability limit 5/s; period 2 s); flow rate 150 $\mu\text{mol/s}$; flash no dark-adapted, flash intensity 7000 $\mu\text{mol/m}^2/\text{s}$, phase 1 flash-length 300 ms, phase 2 flash-length 300 ms, phase 3 flash-length 300 ms, ramp amount 25%; leaf absorptance (abs) 0.84, fraction of absorptance (PS2/1) 0.5; actinic modulation rate 500 Hz.

The fresh biomass was measured after harvest, and the dry biomass was recorded after drying the plants in an 80 °C oven. The water content was calculated as $(W_{\text{fresh}} - W_{\text{dry}}) / W_{\text{fresh}}$ (W_{fresh} : plant fresh biomass; W_{dry} : plant dry biomass). Root tissues were not included in the biomass above. The yield of seed and fruit crops was recorded at the end of the season. The harvested seeds and fruits were also dried in the 80 °C oven to record their dry biomass.

All the crop data were based on the 12 replicate pots in each grow room. Trait data were normalized to facilitate comparison using the control room as the reference (control room was set as 1). A sample *t*-test (two-tailed) was used to compare data groups in statistics.

2.6. The potential for energy savings through solar power modelling

As part of the experimental design, solar windows were not installed on the southern wall (and the eastern end (Room 1) of the greenhouse. We developed a radiation model to estimate the total radiation received should the solar windows be installed in all greenhouse walls. We assumed that the amount of solar energy the solar greenhouse captures is directly related to the amount of electricity it generates; greater exposure to solar radiation of a fully glazed greenhouse leads to higher power generation capacity.

The total amount of solar radiation energy that the greenhouse receives on a given day is dependent on several factors, including the day of the year, altitude, latitude, the slope of the ground the glasshouse sits on, cloud cover, the shape, area, and azimuth angle of the greenhouse, among others. The total radiation that a greenhouse receives can be contributed to beam radiation (direct radiation) and diffused radiation (indirect radiation) (Al-et al., 2020):

$$Q_i = Q_b + Q_d$$

where Q_b is the beam radiation and Q_d is diffuse radiation.

When sky is clear the beam radiation amount that reaches the inclined external surface of the greenhouse in each day can be expressed as²¹:

$$Q_b = \int_{t_1}^{t_2} I_0 T_b \cos \theta dt$$

where t_1 and t_2 are the sunrise and sunset times. I_0 is the radiation intensity that reaches the outer layer of the atmosphere, which varies with the distance between the sun and the earth. I_0 can be formularized as a function to the day of the year as the following where n is the day of the year, where January 1st is 1 and 31st December is 365 (Momoh, 2013).

$$I_0 = 1367 \left(1 + 0.033 \cos \frac{360n}{365} \right)$$

T_b refers to the atmospheric transparency coefficient of the solar beam radiation, which is associated with the local atmosphere volume and atmospheric conditions and can be calculated by an empirical formula described previously (Kreith and Kreider, 1978).

$$T_b = 0.56(\exp(-0.56M_h) + \exp(-0.095M_h))$$

M_h is the gas volume of the atmosphere at the test location under certain conditions. The volume depends on the location altitude a , and the solar altitude angle h ²⁴.

$$M_h = M_0 \left(\frac{288 - 0.0065a}{288} \right)^{5.256}$$

$$M_0 = \begin{cases} \frac{1}{\sin h} & \text{when } h \geq 30^\circ \\ [1229 + (614 \sin h)^2]^{0.5} - 614 \sin h & \text{when } h < 30^\circ \end{cases}$$

The θ is the angle between the beam radiation and the normal line of the inclined greenhouse surface. This angle is closely associated with the solar declination δ , the hour angle t , the slope of the surface ω , the azimuth angle of the surface ϵ , and the latitude of the greenhouse ϕ .

This association can be represented by (Maatallah et al., 2011):

$$\cos \theta = \cos \delta \cos \varphi \cos t \cos \omega + \cos \epsilon \cos \delta \sin \varphi \cos t \sin \omega + \sin \epsilon \cos \delta \sin t \sin \omega + \sin \delta \sin \varphi \cos \omega - \cos \epsilon \sin \delta \cos \varphi \sin \omega$$

The coefficient ϕ is the latitude of the greenhouse where northern hemisphere is positive and southern hemisphere is negative; t is the time angle where t is 0° at local noon, and t changes roughly around 15° per hour and reaches 90° at sunrise and sunset (where in the morning t is negative and in the afternoon is positive); ϵ is the azimuth angle of the greenhouse surface where 0° is facing north, -90° due west, 90° due east, and 180° due south.

The diffuse radiation that reaches the greenhouse inclined surface in each day can be formulated by integral of the hour angle t as following (Liu and Jordan, 1960):

$$Q_d = \int_{t_1}^{t_2} I_0 T_d \sin h \cos \omega / 2^2 dt$$

Here T_d refers to the transparency coefficient of the diffuse radiation. It has a linear relationship with the transparency coefficient of the direct radiation. And h is the solar altitude angle that is determined by geographical latitude ϕ , the solar declination angle δ , the hour angle t , and others. The association may be generalised as²⁷:

$$T_d = 0.271 - 0.294T_b$$

$$\sin h = \sin \varphi \sin \delta + \cos \varphi \cos \delta \cos t$$

When taking the weather into consideration, the radiation is largely affected by the cloud cover. This can be formularized by incorporating the cloud cover coefficient. The beam direction radiation can be calculated following (Ma et al., 2013). CR is the cloud cover ratio ranging from 0 to 100%.

$$Q_b^c = \int_{t_1}^{t_2} (1 - CR) I_0 T_b \cos \theta dt$$

The diffuse component of the radiation with cloud cover is more complicated in cloudy weather and can be calculated by introducing cloud cover coefficient CF (Duffie and Beckman, 2013).

$$Q_d^c = \int_{t_1}^{t_2} CF \left(I_0 T_b \cos \theta + I_0 T_d \sin h \cos \omega / 2^2 \right) dt - Q_b^c$$

The model described above was used to simulate the radiation received by the solar windows (roof, north wall, and west wall of the greenhouse) in Murdoch University. The weather condition was simulated using the latitude, longitude, altitude, daily minimum and maximum temperatures, cloud conditions and solar radiation intensities. Historical weather data, from June 2021 to May 2022, were obtained from Visual Crossing Weather Data & Weather API (<https://www.visualcrossing.com/>), and the daily solar radiation data were collected from Bureau of Meteorology (<http://www.bom.gov.au>) and Solcast (<https://www.solcast.com/>). Simple linear regression was used to investigate the correlation between the simulated radiation and the electricity generated in the Murdoch solar greenhouse.

The radiation data were analysed for the correlation with the monthly electricity production from June 2021 to May 2022. As a result, the estimated radiation was highly correlated with the monthly electricity generation ($r^2 = 0.8043$, $p < 0.0001$) (Extended Data Fig. 3),

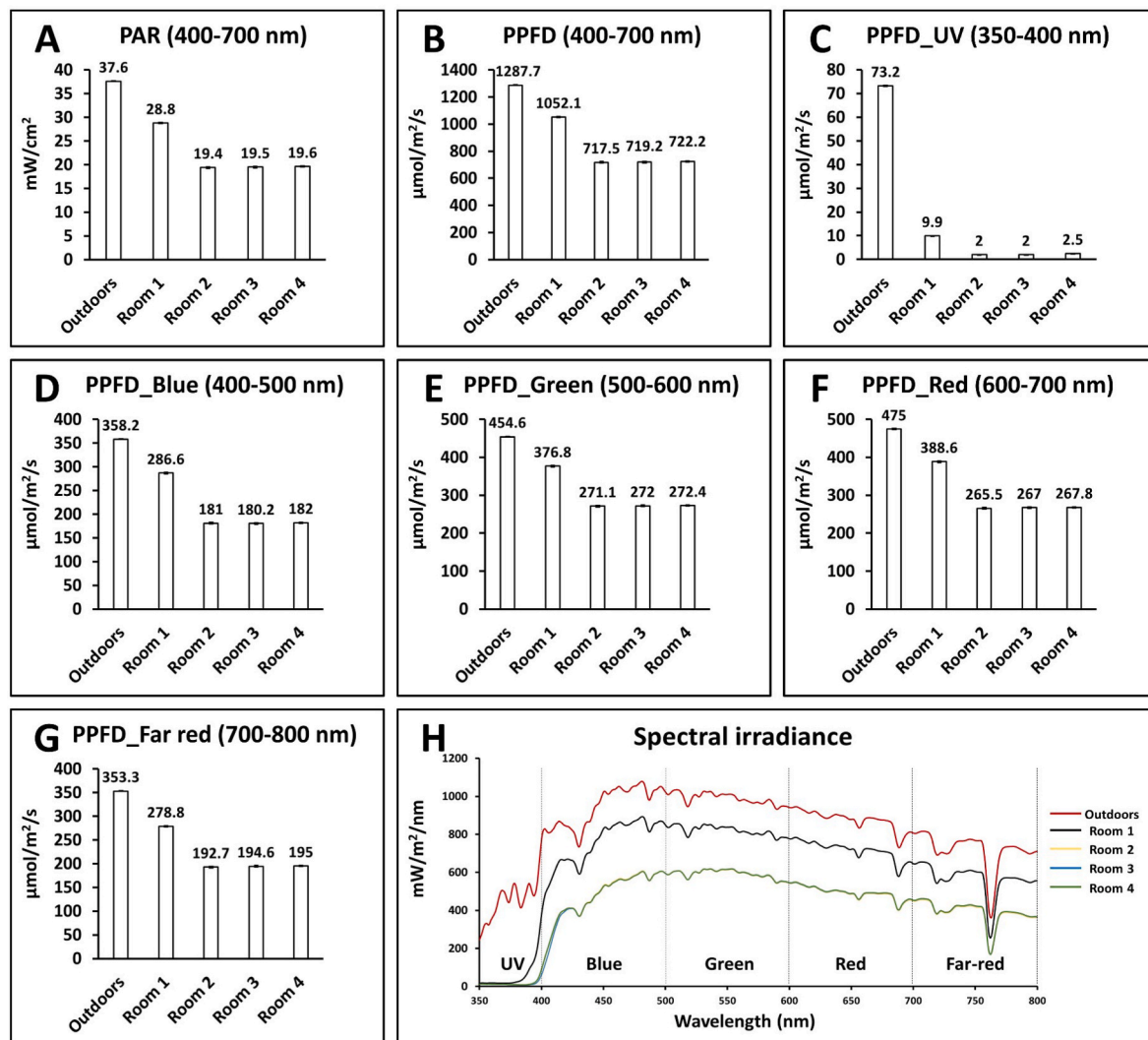


Fig. 3. Comparing the light intensity and quality in the outdoor space, the conventional glass room and the three ClearVue glass rooms. A: Photosynthetically active radiation (PAR) (400–700 nm) in the four growth rooms and the outdoors; B: Photosynthetic Photon Flux Density (PPFD) (400–700 nm) in the four growth rooms and the outdoors; C: PPFD UV range (350–400 nm) in the four growth rooms and the outdoors; D: PPFD blue light range (400–500 nm) in the four growth rooms and outdoors; E: PPFD green light range (500–600 nm) in the four growth rooms and outdoors; F: PPFD red light range (600–700 nm) in the four growth rooms and outdoors; G: PPFD far red light range (700–800 nm) in the four growth rooms and outdoors; H: The spectral irradiance (350–800 nm) distribution measured in the four growth rooms and outdoors.

suggesting that this model can accurately predict the solar power potential in similar solar greenhouses. This model was also used to simulate the radiation received by a solar greenhouse that was fully glazed with solar windows (on the roof, north wall, south wall, west wall, and east wall) in Murdoch (Perth) and eight other geographical locations: Rio de Janeiro (22° 54' 24.6492" S and 43° 10' 22.4256" W), Beijing (39° 54' 15.12" N and 116° 24' 26.6256" E), New Delhi (28° 36' 50.1804" N and 77° 12' 32.4756" E), Los Angeles (34° 3' 8.0424" N and 118° 14' 37.266" W), New York (40° 42' 45.99" N and 74° 0' 21.5028" W), Haifa (32° 47' 38.5656" N and 34° 59' 22.4556" E), and Paris (48° 51' 23.8104" N and 2° 21' 7.9992" E). Historical weather data and the daily solar radiation data on these locations were obtained from Visual Crossing Weather Data & Weather API (<https://www.visualcrossing.com/>), Bureau of Meteorology (<http://www.bom.gov.au>) and Solcast (<https://www.solcast.com/>). In the modelling, the facing angle of the greenhouses in different locations was considered to face directly North for locations in the Southern Hemisphere and face directly South for locations in the Northern Hemisphere, on a flat ground without slope. The resulting monthly radiation data were utilised to estimate the energy generation in these nine locations over 12 months from June 2021 to

May 2022 by a 150 m² fully-glazed solar greenhouse.

The monthly energy production outputs of all individual PV window arrays installed at greenhouse were obtained from the online data logs stored at Enphase website dedicated to Murdoch greenhouse system. Using the detailed system installation diagram describing the geometry and placement of each window array (most of which were parallel connected bundles of 12 windows each) and the production datalogs from each array, it was possible to separate the contributions of each wall and roof area to the total energy production. The details of window array installation locations and the season-dependent energy harvesting behaviours of solar windows installed into different parts of greenhouse building envelope were reported previously (Vasiliev et al., 2023b).

3. Results and discussion

3.1. Energy consumption, generation, and water usage

Before implementing the climate control algorithms in the greenhouse, a thermal insulation performance test revealed that Clearvue-glazed grow rooms maintained higher night temperatures compared to

the control room with plain glass, and solar grow rooms exhibited a slower daytime temperature rise due to differences in solar heat gain and thermal insulation (Vasiliev et al., 2023b). During the twelve months of farming experiments (June 2021 to May 2022), the greenhouse microclimate was strictly controlled in all four grow rooms (temperature at 24 ± 2 °C day time and 18 ± 2 °C night time). The monthly temperature conditions in this period were summarized in Extended Data Table 1 and more detailed daily weather conditions can be found on <https://www.timeanddate.com/>. During this period, the solar grow-rooms consumed 56% (annual average) of the energy used in the conventional room to achieve the same microclimate, primarily due to the reduced solar radiation entering the growth rooms (Fig. 2B). Compared to a typical installation of standard PV panels on an optimally tilted roof area, the solar greenhouse consistently maintained its energy production output, even with the considerable presence of vertically oriented windows on the North and West Walls (Vasiliev et al., 2023b). The average daily electricity harvested was around 17 kWh from three solar rooms on sunny days (Extended Data Table 3). The monthly solar power production per room ranged from 101 (July 2021) to 178 kWh (December 2021), depending on the varied solar radiation intensity during different seasons (Fig. 2C). Solar energy offset approximately 24% (annual average) of the total energy usage in solar growth rooms. In an one-year period from June 2021 to May 2022, the average net electricity imported from grid to a solar room was 5727 kWh, while the net electricity to the normal room was 13344 kWh (Extended Data Table 3). Thus, solar greenhouse reduced the long-term average energy consumption by 57% (Fig. 2 D; Extended Data Table 3) due to a combination of energy production and saving. The weather conditions observed over these twelve months are representative of Western Australia's typical climate patterns. Additionally, stringent temperature control measures were implemented in the solar greenhouse for research purposes, ensuring representative energy consumption across different months in a year. As a result, the energy offset findings are highly reliable and replicable. Solar rooms have also demonstrated significant water-saving benefits in farming production. Soil moisture content was being reduced by 1.91% daily in a conventional glass room when growing lettuce (variety Green Cos) in March 2022 (daytime highest temperature was from 34 °C to 38 °C, and lowest at 9 °C at night (<https://www.timeanddate.com/>)). In comparison, soil moisture was reduced by 1.35% in solar growth room, resulting in a 29% water saving (Fig. 2 A and Extended Data Table 4).

3.2. Light quantity and quality in the ClearVue solar greenhouse

The direct VLT was approximately 80% in conventional rooms and 55% in solar rooms (lower than the solar glass direct VLT of 70% due to the greenhouse structure), leading to a reduction of approximately 30% in the direct-beam light intensity within the solar rooms due to a portion of the sunlight being reflected or captured to generate electricity (Fig. 3A and B). Different wavelengths had different transmittance through the solar glass. Approximately 50%–51% of the photosynthesis-effective blue light (400–500 nm), 60% of the green light (500–600 nm), 55% of red light (600–700 nm), and 55% of far-red light (700–800 nm) were retained in the solar growth rooms compared to the outdoor conditions, compared with 63%–64% of blue light, 72% of green light, 69% of red light, and 69% of the far-red light in the conventional room (Fig. 3D–G).

Meanwhile, 97% of the photosynthetically damaging UV light (350–400 nm) was intercepted by the PV panels in the solar rooms, compared to 86% intercepted by the conventional greenhouse glass (Fig. 3 C). The spectral irradiation patterns in the greenhouse and outdoors were identical from visible to the far-red light, and the light intensity distribution was the main difference in this wavelength range (Fig. 3D–H).

3.3. Crops production in solar greenhouse

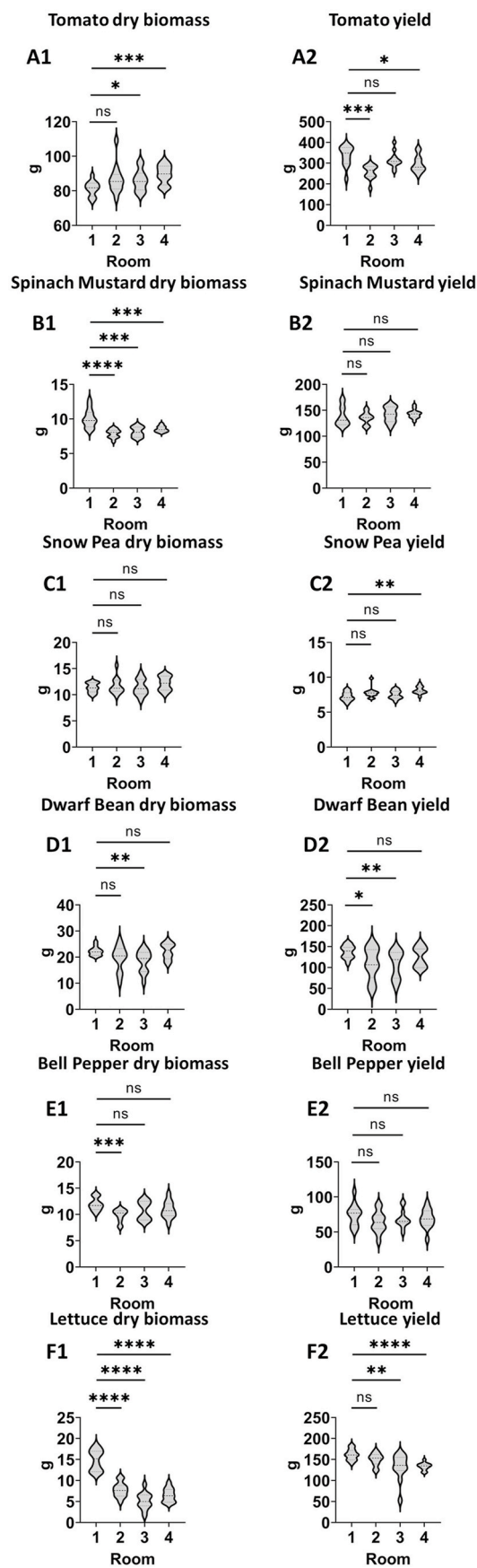
A comprehensive assessment of farming production in the solar greenhouse involved eighteen crops cultivated over two growth seasons (Extended Data Table 2). Common greenhouse-growing horticulture crops maintained the same or higher productivity in the solar greenhouse environment as those grown in the conventional greenhouse. Six crops, including tomato, lettuce, spinach mustard, dwarf bean, bell pepper and sweet corn, produced the same levels of fresh biomass in at least one of the solar rooms as in the conventional greenhouse. At the same time, chilli plants had 19%–22% more fresh biomass in solar rooms than those grown in the conventional greenhouse (Extended Data Fig. 4). Six crops had no significant difference in dry biomass in at least one solar room, including bell pepper, dwarf bean, snow pea, tomato, canola, and sweet corn. Tomato and chilli crops had 10% and 14% more dry biomass, respectively, when grown in solar rooms. Common horticulture crops, eg., lettuce, spinach mustard, basil, spring onion, chilli, bell pepper, and sweet corn, had higher water content in solar grow rooms by 1%–9% (Extended Data Fig. 5).

Common horticulture crops, such as tomato, dwarf bean, chickpea, lettuce, spinach mustard, and bell pepper, maintained the same yield level in the solar room as those in the conventional room. At the same time, snow peas had a 12% yield increase in the solar rooms (Fig. 4 and Extended Data Fig. 4). Across the three solar rooms with different fluorescent interlayer compositions, most crops did not differ significantly in biomass and yield, while several crops (e.g. basil and chickpea), had better productivity in Room 4. Broadacre crops, such as barley, wheat, lupin, and sunflower, experienced a notable decline in biomass and yield or even failed to reach maturity when grown in the solar rooms. The full detailed biomass and yield data of all tested crops are shown in Extended Data Fig. 4.

Compared with the other two solar rooms, the glazing system design used in Room 4 had higher transmittance in the UV, blue and green light ranges, leading to increased biomass and yield along with reduced SAS for some crops. Thus, continuing to refine the solar window's light transmittance profile presents an ongoing opportunity to enhance its potential for optimal crop production. Plants use red and blue light more efficiently for photosynthesis than green light because of the low absorbance of the green light (Singh et al., 2015; Virtanen et al., 2022). The green light had the highest transmittance through the solar glass, which also efficiently reflected all infrared wavelengths above 1000 nm. Therefore, future fluorescent and scattering interlayers and optical coatings can be designed to direct more green light for energy generation while transmitting (or emitting) more blue and red light for plant growth. This can be achieved by incorporating green-light wavelength-selective layers to enhance green light absorbance (followed by red or near-IR fluorescence that can be partially trapped in glazings) and improve the power conversion efficiencies in the green-light region. However, recent studies also showed that red and blue light have lower quantum efficiency in photosynthesis than green light at higher PPFD, because more green light was able to penetrate through the upper leaves and increase photosynthesis in the lower canopy, while much of the high-intensity red and blue light was dissipated as heat (Liu et al., 2021; Kim et al., 2004). Thus, further study should clarify the optimal fractioning of light for energy generation and plant growth in the solar greenhouse environment, which would vary by crops' species and cultivars based on their plant architecture.

3.4. Crops growth, development, and photosynthesis in solar greenhouse

The crops were monitored on their growth and development in the solar greenhouse. The filtered lighting environments had expectedly a neglectable influence on seed germination. Both germination rate and germination speed did not differ significantly for crops planted in solar or conventional rooms, except for a slightly delayed germination for bell pepper and spring onion (Extended Data Fig. 6 and Extended Data



(caption on next column)

Fig. 4. Comparing the dry biomass and yield of six commercial crops in the conventional glass room (Room 1) and the three solar glass rooms (Rooms 2 to 4). The yield data referred to the edible and marketable part of fresh biomass. The p values between solar and conventional rooms were calculated by a two-tailed Student's t-test: *p < 0.05; **p < 0.01; ***p < 0.001; ****p < 0.0001; ns indicates no significance. Tomato and lettuce data are from season 2 (March–September 2022).

Table 5). Twelve crops exhibited shade-avoidance syndromes (SAS) at seedling stage, including longer hypocotyls, smaller leaves, and increased height in the solar rooms (Extended Data Figs. 7 and 8). However, SAS were less severe in solar Room 4 for several crops, including chickpea and lettuce seedlings. Despite SAS in the seedling stage, the six commercial crops widely grown in the greenhouse were adapted to the changed light conditions in the solar rooms by growing taller with up to 19% larger and/or up to 22% more leaves in vegetative growth stage (Fig. 5 and Extended Data Figs. 9 and 10). Development and flowering were generally delayed 3–17 days in solar rooms, except for sunflower, dwarf bean and chilli (Extended Data Fig. 11).

Physiologically, five out of six greenhouse commercial crops maintained the same level of leaf chlorophyll content (CHL) in the solar rooms, except dwarf bean. Dwarf bean increased CHL by 6%–13% in solar rooms (Extended Data Figs. 12 and 13). Most crops, except wheat, lettuce and sweet corn, had increased actual light use efficiency and leaf health in solar rooms with increased ΦPSII (actual quantum yield of PSII in light-adapted leaves) and Fv/Fm (maximum quantum efficiency of photosystem II, PSII) (Extended Data Fig. 13). All the crops, except bell pepper, had significantly decreased electron transport rate (ETR) by 23%–68%. The levels of stomatal conductance and transpiration rate in solar growth rooms depended on the crops species and varieties (Extended Data Fig. 13). The full detailed growth and photosynthesis data are shown in Extended Data Figs. 6, 7, 9, 11, and 13.

In our study, the filtered light condition in solar greenhouse negatively affected some crops, inducing the SAS, delayed flowering time and reduced biomass. Typical SAS is detrimental to the seedling growth. The excessive hypocotyl elongation resulted in poor seedling establishment and susceptibility to early-stage lodging and diseases (Yang and Li, 2017). Apart from the seedling stage, some crops also show SAS in vegetative growth stage (tomato and lettuce in this study). Therefore, preventing SAS is critical to improve the crop performance in the solar greenhouse. Horticultural practices and commercial LED supplementary lighting are used to minimize seedling SAS (Song et al., 2019). It has been demonstrated that the lower temperature and a higher red/far-red ratio by supplementing red light effectively mitigate crops SAS in the greenhouse (Yang and Li, 2017; Casal and Fankhauser, 2023; Patel et al., 2013). Another promising strategy is to develop crop varieties with reduced SAS by inducing genetic mutations, followed by selective breeding. This approach has been used on several different crops to mitigate their SAS (Wille et al., 2017; Sessa et al., 2018). A future innovative solution to reduce SAS in shaded solar greenhouses is to manipulate the genes that are involved in the light-mediated hypocotyl growth, such as sensory photoreceptors, PIFs, and auxin perception genes (Leivar et al., 2009, 2012), thus enhancing the crop's adaptability to low-light conditions.

Meanwhile, we observed several crops displayed shade tolerance in the solar greenhouse by growing larger leaves to capture more sunlight for photosynthesis in the shade. The larger leaf area in solar rooms increased the overall photosynthesis surface area, leading to comparable dry biomass with conventional glass rooms. The size of leaves is through the control of both cell proliferation and cell expansion throughout the stages of leaf development. These processes are under stringent control by an array of integrated signals from the plant's internal regulatory network and the surrounding growth environment. Several genes have been shown to positively regulate leaf size by increasing cell number (AVP1, GRF5, JAW, BRI1, GA20OX1, etc.) or cell length (EBP1, EXI, EXP10, SAUR19, etc.) (Gonzalez et al., 2010; Gonzalez and Inze, 2015).

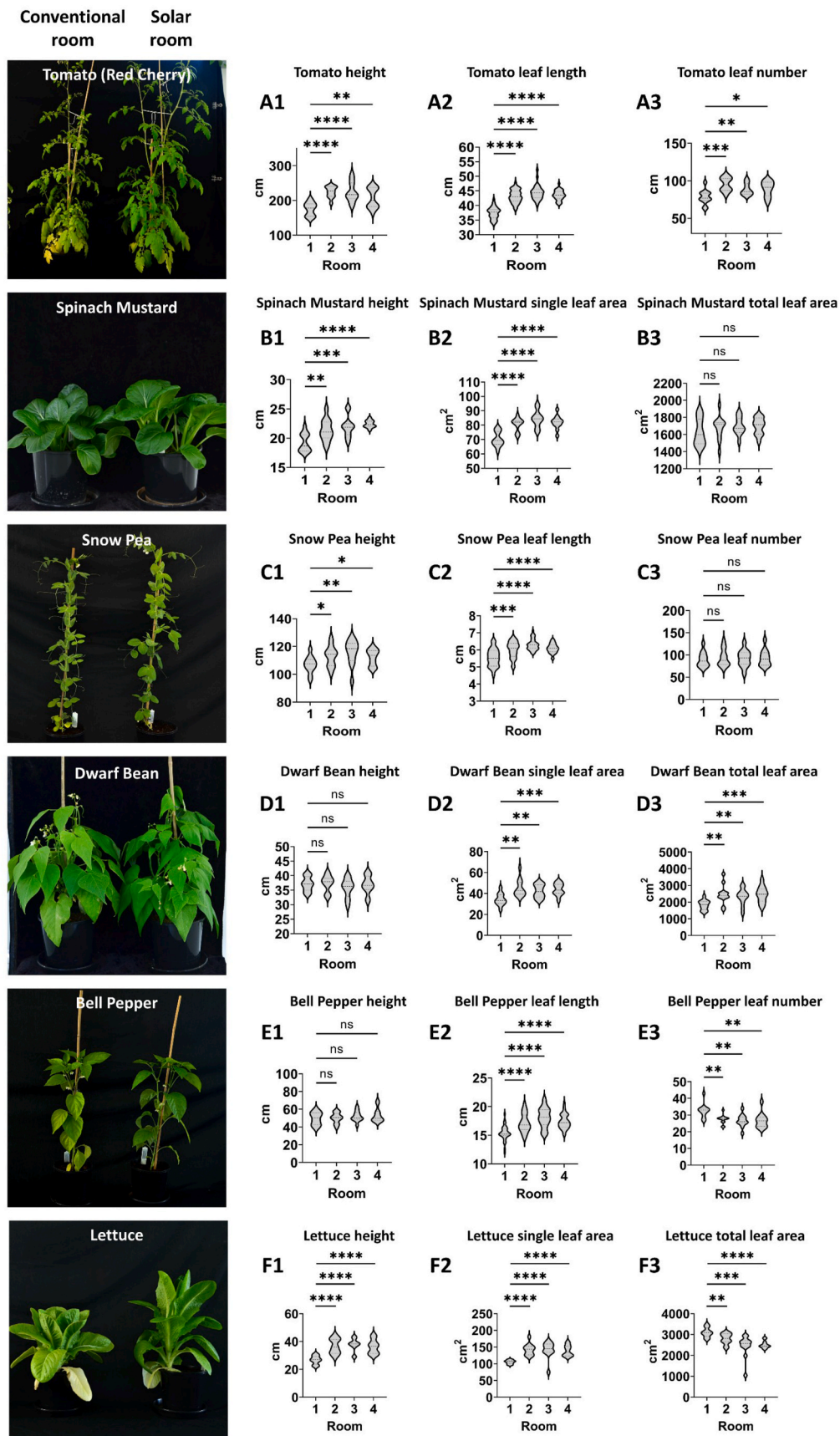


Fig. 5. Comparing the vegetative growth of six commercial crops in the conventional glass room (Room 1) and three solar glass rooms (Rooms 2 to 4). The p values between solar and conventional rooms were calculated by two-tailed *t*-test: **p* < 0.05; ***p* < 0.01; ****p* < 0.001; *****p* < 0.0001; ns indicates no significance. Tomato and lettuce data from season 2.

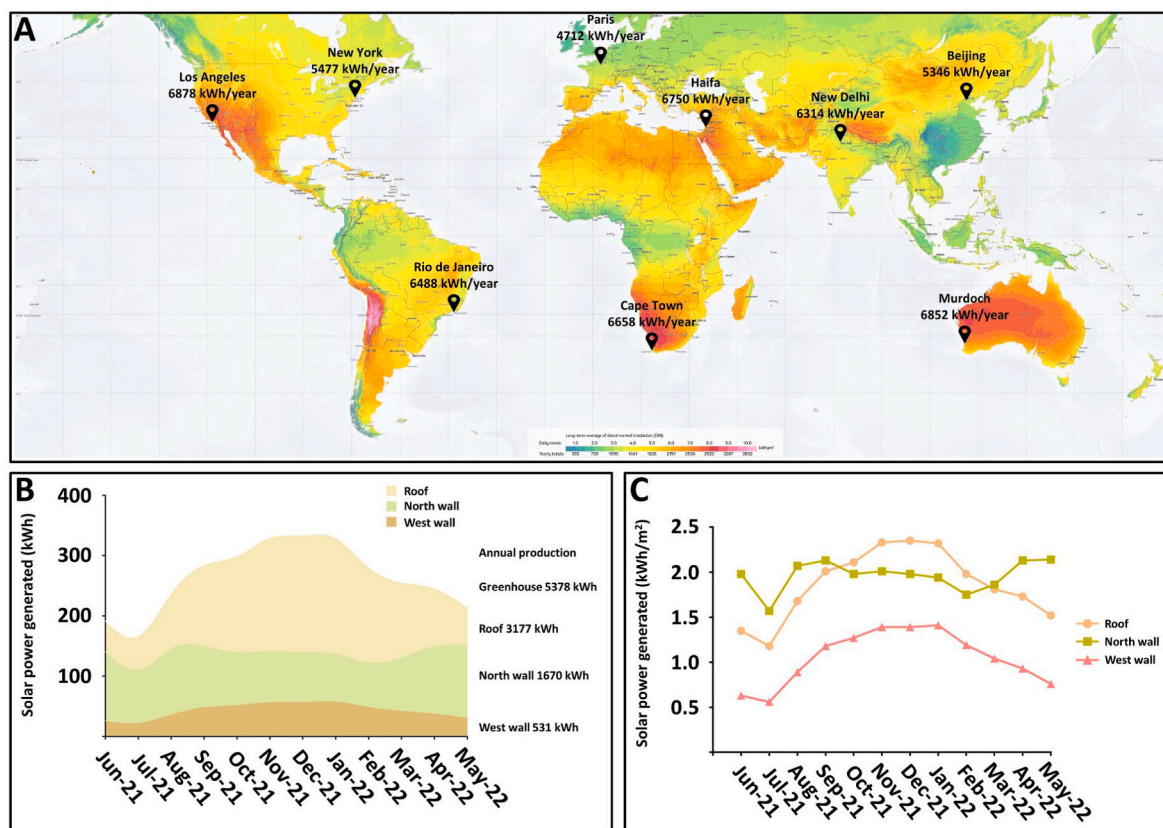


Fig. 6. Solar greenhouse global energy potential and electricity production capacity of clear solar windows mounted at different tilt angles and orientations. A: Solar greenhouse global annual photovoltaic energy potential (per 150 m² of land footprint area) in diverse geographic locations on a world's direct solar irradiation map. The annual electricity generation figures in different cities are estimated based on a 150 m² fully-glazed solar greenhouse using our model. The direct irradiation map is sourced from Global Solar Atlas: <https://globalsolaratlas.info/about/>; B: Analyzing and comparing the monthly solar energy production (kWh) from both the roof and side walls of the Murdoch solar greenhouse; C: Analyzing and Comparing the monthly solar energy production in unit solar window area (kWh/m²) from both the roof and side walls of the Murdoch solar greenhouse.

Thus, for those crops with lower biomass yields in the solar rooms, developing a new “large-leaf” variety through manipulating these regulating genes may enhance their ability to thrive in solar greenhouses. However, this strategy needs further investigation because larger leaves may increase the overlapping of leaves in commercial production, therefore limiting the plant density and productivity per unit.

For crop types not covered in our study, several approaches can be taken to evaluate their performance in a solar greenhouse. One of the approaches was to include additional crops in the future test, especially those with varying light, temperature, and humidity requirements. This will provide more data on the adaptability of different crop types to solar greenhouse conditions. Another approach was to use crop simulation models to predict the performance of untested crops based on their known physiological and growth parameters. For this approach, it is essential to adjust the model to reflect the specific environmental conditions within the solar greenhouse. Another effective approach is to collaborate with greenhouse technology experts to identify the likely performance of untested crops and the adjustments needed for their successful cultivation.

3.5. Energy potential of solar greenhouse in diverse geographic locations

As part of the experimental design, solar windows were not installed on the southern (back) wall and the eastern end of the greenhouse (Fig. 1), which led to a decrease in the amount of electricity generated through solar power and underestimated the potential savings in energy. Our radiation model was based on an assumption that the amount of

solar radiation the greenhouse receives is directly related to the amount of power it produces. The result of the model suggested that the total solar radiation received by a fully glazed solar greenhouse would increase the energy output by 27% annually, from 5379 kWh to 6852 kWh. Using the radiation model, annual electricity output of 6300–6800 kWh would be generated if the solar greenhouse (with a total floor area of 150 m² and fully equipped with solar windows) was constructed in Cape Town, Haifa, Los Angeles, New Delhi, or Rio de Janeiro. The same solar greenhouse would generate less electricity if it were in Beijing, New York, or Paris at 4700 to 5400 kWh annually (Fig. 6A). In such locations with lower solar radiation, it would be expected to consume less energy for cooling in summer months but more energy for heating in winter season. The energy offset from solar roofs and facades in these locations needs further investigation.

The energy production data (June 2021 to May 2022) from Enphase Envoy interface was used to compare the PV yield of roof-based and wall-based windows. The result showed that the roof-based windows (north-facing, tilted at a 20-degree angle to the horizontal) produced 59% of the total annual output, while north wall-based windows generated 31% and west wall-based (only 21 windows in total) contributed 10% (Fig. 6B). The highest monthly electricity generation from roof-based windows occurred in December, reaching 334 kWh, whereas the lowest was recorded in July at 167 kWh. Compared with the roof, the north wall production exhibits a noteworthy feature with its relative insensitivity to seasonal solar intensity and geometry variations, ranging from 111 kWh/month (May) to 152 kWh/month (July). During a number of months (from March to September), the vertical north wall produced even more electricity than the optimally-tilted roof per unit

window area (Fig. 6C), which shows a notable energy harvesting behavior difference, in comparison with conventional PV systems. The seasonal variations of the west wall energy production were similar to those observed from the roof area, but yielding obviously less electricity (Fig. 6B and C).

Our solar greenhouse has four distinct grow rooms separated by insulated panels to establish uniformity for experimental purposes. A preparatory room was situated at the rear of the greenhouse to facilitate research activities. This configuration led to a reduction of natural light entering through the side windows and underestimated the capacity of the greenhouse to generate electricity. The exclusion of side walls in the PV installation also reduced the sunlight into the solar rooms. Additionally, this design choice may have impacted the overall light distribution within the solar rooms, potentially influencing both crop growth and energy generation. This limitation should be carefully considered when interpreting the results. Future studies could address this limitation by incorporating side walls into the PV system or by evaluating alternative configurations that maximize both natural light entry and electricity generation. This would provide a more comprehensive understanding of the greenhouse's full potential and offer insights into design optimizations for improved performance.

It is worth noting that energy consumption was high in our design due to the stringent temperature control measures applied within the solar greenhouse for research purposes. The temperature control would be more flexible, adaptable and efficient in a productive commercial greenhouse setting. A recent study showed that achieving optimum environmental conditions for bell pepper production in a greenhouse costs 62 kWh/m²/year in Australia, using a gas hot water system for heating and pad and fan system for cooling (Samaranayake et al., 2020). Our two growing seasons experiment suggested that only 56% of the total energy (35 kWh/m²/year) was required to maintain the same climate variables compared to traditional greenhouse systems in regions with a similar climate. In this scenario, thus, the solar greenhouse located in Perth could entirely offset its consumption with the capacity of generating 46 kWh/m²/year. Solar greenhouses in various locations were found to produce over 35 kWh/m²/year of energy, except Paris (Fig. 6). This indicates that solar greenhouses in these regions have the potential to fully offset their energy consumption. However, the exact energy consumption of these greenhouses is not yet well-defined, further research is needed to clarify this. In addition, the radiation model we used in this study had some limitations because in reality, apart from solar radiation, other factors can also influence energy output, such as temperature and solar glasses age.

The economic feasibility of scaling solar greenhouses depends on initial investment costs and long-term returns. Although the initial investment is higher than traditional greenhouses, solar greenhouses can lead to substantial operational savings, mainly by generating their own power to reduce reliance on grid electricity or fossil fuels, lowering energy bills for heating, cooling, and lighting. Our result showed that the solar greenhouses had a potential to be 100% self-sustainable in different geographic locations around the world. In addition, solar greenhouses offer the benefit of lower resource consumption, particularly reduced water usage, which is especially valuable in arid regions like the Middle East. Advances in solar technology and decreasing costs of photovoltaic materials further enhance the potential for solar greenhouses to become a cost-effective and scalable solution for sustainable agriculture. These benefits also have a significant positive impact on global carbon reduction goals. To keep global warming to no more than 1.5 °C, many countries have set ambitious carbon neutrality targets as part of international agreements. Solar greenhouses can help these nations achieve their goals by cutting emissions from the agriculture sector. Governments can align the agricultural sector with national climate targets while also ensuring food security and advancing sustainability, by integrating renewable energy and energy-efficient technologies into agricultural practices. The payback period for solar greenhouses can vary depending on location, scale, and local energy

costs, but in the long term, solar greenhouses can have a positive return on investment (ROI), by energy and resource savings, and increased resilience to climate change. The increasing consumer demand for sustainably grown, locally sourced, and organic food also contributes to the economic feasibility of solar greenhouses.

4. Conclusions

Agriculture production is energy intensive. Solving the food, energy, and environment trilemma is an energy challenge (Tilman et al., 2009). Transforming the food production systems will require a transformation of our energy system. In this study, we designed and built a research-scale greenhouse using high-transparency window-integrated PV as the roof and window materials.

1. We demonstrated that the use of window and roof-integrated photovoltaics has significant potential to improve the sustainability of greenhouse farming, with substantial energy and water saving.
2. Crops commonly grown commercially through greenhouse farming demonstrated robust growth without yield loss in the solar greenhouse.
3. Across a range of global locations in the world's agricultural continents, solar greenhouses have potential to yield sufficient energy to fully offset the energy consumption in a commercial greenhouse setting with adaptable and efficient temperature control methods.

Future advancement on light transmittance profile optimisation of the photovoltaic windows and flexible, adaptable, and efficient temperature control techniques could allow the solar greenhouses being able to entirely offset their energy consumption and becoming a zero-emissions food production system on a global scale. Solar greenhouses offer a multifaceted set of real-world benefits that address critical challenges in modern agriculture, including energy consumption, resource management, climate resilience, and food security.

CRedit authorship contribution statement

Hao Luo: Writing – original draft, Methodology, Investigation, Formal analysis, Data curation. **Mikhail Vasiliev:** Investigation, Data curation. **Tianhua He:** Writing – review & editing, Formal analysis. **Penghao Wang:** Software, Formal analysis. **Jamie Lyford:** Supervision, Funding acquisition. **Victor Rosenberg:** Funding acquisition, Conceptualization. **Chengdao Li:** Writing – review & editing, Resources, Funding acquisition, Conceptualization.

Data availability

The data that support the findings of this study are available on request from the corresponding author.

Declaration of competing interest

The ClearVue glasshouse is designed and manufactured by ClearVue Technologies Limited and Mikhail Vasiliev, Jamie Lyford and Victor Rosenberg are the company employee.

Acknowledgement

This study was financially supported by Cooperative Research Centres Projects (CRC-P) Grants (IRMA ID#20727: ICG001945) and ClearVue Technologies Limited.

Appendix A. Supplementary data

Supplementary data to this article can be found online at <https://doi.org/10.1016/j.clet.2025.100895>.

Data availability

Data will be made available on request.

References

- Al-Helal, I., Alsadon, A., Shady, M., Ibrahim, A., Abdel-Ghany, A., 2020. Diffusion characteristics of solar beams radiation transmitting through greenhouse covers in arid climates. *Energies* 13.
- Alghamedi, R., Vasiliev, M., Nur-E-Alam, M., Alameh, K., 2014. Spectrally-selective all-inorganic scattering luminophores for solar energy-harvesting clear glass windows. *Sci Rep-Uk* 4.
- Calicioglu, O., Flammini, A., Bracco, S., Bellu, L., Sims, R., 2019. The future challenges of food and agriculture: an integrated analysis of trends and solutions. *Sustain.-Basel* 11.
- Casal, J.J., Fankhauser, C., 2023. Shade avoidance in the context of climate change. *Plant Physiol.* 191, 1475–1491.
- Cossu, M., Yano, A., Li, Z., Onoe, M., Nakamura, H., Matsumoto, T., et al., 2016. Advances on the semi-transparent modules based on micro solar cells: first integration in a greenhouse system. *Appl. Energy* 162, 1042–1051.
- Costa, C., Wollenberg, E., Benitez, M., Newman, R., Gardner, N., Bellone, F., 2022. Roadmap for achieving net-zero emissions in global food systems by 2050. *Sci Rep-Uk* 12.
- Djevic, M., Dimitrijevic, A., 2009. Energy consumption for different greenhouse constructions. *Energy* 34, 1325–1331.
- Duffie, J.A., Beckman, W.A., 2013. *Solar Engineering of Thermal Processes*, 4. Solar Engineering of Thermal Processes, pp. 1–910.
- Gavrila, S., Gontean, A., 2010. Greenhouse energy balance modeling review and perspectives. 10th Ifac Workshop on Programmable Devices and Embedded Systems (Pdes 2010), pp. 162–166.
- Golasa, P., Wysokinski, M., Bienkowska-Golasa, W., Gradziuk, P., Golonko, M., Gradziuk, B., et al., 2021. Sources of greenhouse gas emissions in agriculture, with particular emphasis on emissions from energy used. *Energies* 14.
- Gonzalez, N., Inze, D., 2015. Molecular systems governing leaf growth: from genes to networks. *J. Exp. Bot.* 66, 1045–1054.
- Gonzalez, N., De Bodt, S., Sulpice, R., Jikumaru, Y., Chae, E., Dhondt, S., et al., 2010. Increased leaf size: different means to an end. *Plant Physiol.* 153, 1261–1279.
- Kim, H.H., Goins, G.D., Wheeler, R.M., Sager, J.C., 2004. Green-light supplementation for enhanced lettuce growth under red- and blue-light-emitting diodes. *Hortscience* 39, 1617–1622.
- Kreith, F., Kreider, J.F., 1978. *Principles of Solar Engineering*. Hemisphere Pub. Corp., Washington.
- Laborde, D., Mamun, A., Martin, W., Pineiro, V., Vos, R., 2021. Agricultural subsidies and global greenhouse gas emissions. *Nat. Commun.* 12.
- Leivar, P., Tepperman, J.M., Monte, E., Calderon, R.H., Liu, T.L., Quail, P.H., 2009. Definition of early transcriptional circuitry involved in light-induced reversal of PIF-imposed repression of photomorphogenesis in young arabidopsis seedlings. *Plant Cell* 21, 3535–3553.
- Leivar, P., Monte, E., Cohn, M.M., Quail, P.H., 2012. Phytochrome signaling in green arabidopsis seedlings: impact assessment of a mutually negative phyB-PIF feedback loop. *Mol. Plant* 5, 734–749.
- Li, Z., Yano, A., Cossu, M., Yoshioka, H., Kita, I., Ibaraki, Y., 2018. Shading and electric performance of a prototype greenhouse blind system based on semi-transparent photovoltaic technology. *J. Agric. Meteorol.* 74, 114–122.
- Liu, B.Y., Jordan, R.C., 1960. The interrelationship and characteristic distribution of direct, diffuse and total solar radiation. *Sol. Energy* 4, 1–19.
- Liu, J., van Iersel, M.W., 2021. Photosynthetic physiology of blue, green, and red light: light intensity effects and underlying mechanisms. *Front. Plant Sci.* 12.
- Ma, C., Zhao, S., Cheng, J., Wang, N., Jiang, Y., Wang, S., et al., 2013. On establishing light environment model in Chinese solar greenhouse. *J. Shenyang Agric. Univ.* 44, 513–517.
- Maatallah, T., El Alimi, S., Ben Nassrallah, S., 2011. Performance modeling and investigation of fixed, single and dual-axis tracking photovoltaic panel in Monastir city, Tunisia. *Renew. Sustain. Energy Rev.* 15, 4053–4066.
- Momoh, M., 2013. Evaluation of clearness index of sokoto using estimated global solar radiation. *IOSR J. Environ. Sci. Toxicol. Food Technol.* 5, 51–54.
- Moor, D., Rosenberg, V., Vasiliev, M., 2022. High-transparency clear glass windows with large PV energy outputs. In: Belis, J., Bos, F., Louter, C. (Eds.), *Challenging Glass Conference; 2022*; Ghent: Challenging Glass.
- Panchasara, H., Samrat, N.H., Islam, N., 2021. Greenhouse gas emissions trends and mitigation measures in Australian agriculture sector-A review. *Agriculture-Basel* 11.
- Paris, B., Vandorou, F., Balafoutis, A.T., Vaiopoulos, K., Kyriakarakos, G., Manolagos, D., et al., 2022. Energy use in greenhouses in the EU: a review recommending energy efficiency measures and renewable energy sources adoption. *Appl Sci-Basel* 12.
- Patel, D., Basu, M., Hayes, S., Majláth, I., Hetherington, F.M., Tschaplinski, T.J., et al., 2013. Temperature-dependent shade avoidance involves the receptor-like kinase ERECTA. *Plant J.* 73, 980–992.
- Ravishankar, E., Booth, R.E., Saravitz, C., Sederoff, H., Ade, H.W., O'Connor, B.T., 2020. Achieving net zero energy greenhouses by integrating semitransparent organic solar cells. *Joule* 4, 490–506.
- Ravishankar, E., Charles, M., Xiong, Y., Henry, R., Swift, J., Rech, J., et al., 2021. Balancing crop production and energy harvesting in organic solar-powered greenhouses. *Cell Rep Phys Sci.* 2.
- Samaranayake, P., Liang, W.G., Chen, Z.H., Tissue, D., Lan, Y.C., 2020. Sustainable protected cropping: a case study of seasonal impacts on greenhouse energy consumption during capsicum production. *Energies* 13.
- Sessa, G., Carabelli, M., Possenti, M., Morelli, G., Ruberti, I., 2018. Multiple pathways in the control of the shade avoidance response. *Plants-Basel* 7.
- Singh, D., Basu, C., Meinhardt-Wollweber, M., Roth, B., 2015. LEDs for energy efficient greenhouse lighting. *Renew. Sustain. Energy Rev.* 49, 139–147.
- Song, J.L., Cao, K., Hao, Y.W., Song, S.W., Su, W., Liu, H.C., 2019. Hypocotyl elongation is regulated by supplemental blue and red light in cucumber seedling. *Gene* 707, 117–125.
- Summers, H.M., Sproul, E., Quinn, J.C., 2021. The greenhouse gas emissions of indoor cannabis production in the United States. *Nat. Sustain.* 4, 644–650.
- Thompson, E.P., Bombelli, E.L., Shubham, S., Watson, H., Everard, A., D'Ardes, V., et al., 2020. Tinted semi-transparent solar panels allow concurrent production of crops and electricity on the same cropland. *Adv. Energy Mater.* 10.
- Tilman, D., Socolow, R., Foley, J.A., Hill, J., Larson, E., Lynd, L., et al., 2009. Beneficial biofuels—the food, energy, and environment trilemma. *Science*. 325, 270–271.
- Vasiliev, M., Rosenberg, V., Goodfield, D., Lyford, J., Li, C., 2023a. High-transparency clear window-based agrivoltaics. *Sust Build* 6.
- Vasiliev, M., Rosenberg, V., Lyford, J., Goodfield, D., 2023b. Field performance monitoring of energy-generating high-transparency agrivoltaic glass windows. *Technologies* 11, 95.
- Virtanen, O., Constantinidou, E., Tyystjärvi, E., 2022. Chlorophyll does not reflect green light – how to correct a misconception. *J. Biol. Educ.* 56, 552–559.
- Wille, W., Pipper, C.B., Rosenqvist, E., Andersen, S.B., Weiner, J., 2017. Reducing shade avoidance responses in a cereal crop. *Aob Plants*. 9.
- Yang, C.W., Li, L., 2017. Hormonal regulation in shade avoidance. *Front. Plant Sci.* 8.
- Yano, A., Onoe, M., Nakata, J., 2014. Prototype semi-transparent photovoltaic modules for greenhouse roof applications. *Biosyst. Eng.* 122, 62–73.